The Journal of Experimental Biology 216, 2619-2631

doi:10.1242/jeb.080705

RESEARCH ARTICLE

High-frequency electrical stimulation reveals a p38–mTOR signaling module correlated with force–time integral

Jill A. Rahnert and Thomas J. Burkholder*

School of Applied Physiology, Georgia Institute of Technology, 555 14th Street NW, Atlanta, GA 30332-0356, USA

*Author for correspondence (thomas.burkholder@hps.gatech.edu)

SUMMARY

High-frequency electrical stimulation (HFES) leads to muscle hypertrophy, and attention has been drawn to the high forces involved. However, both mechanical and metabolic stresses occur simultaneously, and both stimuli influence signaling cascades related to protein synthesis. This study aimed to identify the immediate signaling correlates of contraction-induced force and metabolic stresses under the hypothesis that HFES induces growth-related signaling through mechanical stimulation. Force–time integral (FTI) signaling in mouse tibialis anterior muscle was examined by separately manipulating the time of contraction to emphasize the metabolic aspect or the force of contraction to emphasize the mechanical aspect. When FTI was manipulated by changing the total time of activation, phosphorylation of p54 JNK, ERK and p70S6k$^{T421/S424}$ was independent of FTI, while phosphorylation of acetyl-CoA carboxylase and p38 correlated with FTI. When FTI was manipulated by changing the force of contraction, p54 JNK, ERK and p70S6k$^{T421/S424}$ were again independent of FTI, while phosphorylation of p38 and FAK correlated with FTI. Factor analysis identified a p38–mTOR signaling module that correlated with FTI in both experiments. The consistent link among p38, mTOR and FTI suggests that they form a connected signaling module sensitive to the mechanical aspects of FTI, separate from markers of metabolic load.

Key words: hypertrophy, mTOR, mitogen activated protein kinase, skeletal muscle.

Received 27 September 2012; Accepted 12 March 2013

INTRODUCTION

Skeletal muscle rapidly adapts to demands imposed by physical activity *via* complex processes including increased protein synthesis, activation of satellite cells and changes in gene regulation (Adams et al., 2002; Bodine et al., 2001; Wong and Booth, 1990). Physical activity, including high force contraction (HFC), imposes both mechanical and metabolic stresses that contribute to the biochemical and molecular phenotype of muscle through activation of diverse signaling cascades. Repeated bouts of HFC result in muscle hypertrophy and have been linked to growth-related signaling cascades *via* growth-factor-independent mechanisms (Hornberger and Chien, 2005; Spangenburg et al., 2008). Changes in similar cascades are seen following perturbations of energy metabolism by high-protein feeding, glucose infusion or treatment with the AMP mimetic 5-aminoimidazole-4-carboxamide ribonucleotide (AICAR) (Miyazaki and Esser, 2009). Thus, a specific gap in our understanding of the response of muscle to HFC is the relative role of mechanical and metabolic signaling in activation of growth-related signaling cascades.

The hypertrophic response to HFC is closely coupled to activation of the mammalian target of rapamycin (mTOR) (Spangenburg, 2009). The complex of mTOR with Regulatory Associated Protein of mTOR (RAPTOR) is known as mTORC1 and phosphorylates the eIF4E binding protein (4EBP) and p70S6 kinase to increase protein synthesis. Muscle overload results in rapamycin-sensitive activation of mTOR targets and muscle hypertrophy (Bodine et al., 2001; Goodman et al., 2011), and acute phosphorylation of p70S6k on T389 by mTORC1 is predictive of long-term adaptive changes in mass following HFC training (Baar and Esser, 1999). Activity of mTORC1 depends on the GTPase Rheb, and phosphorylation of TSC2, the Rheb-GAP, by Akt, p38 or ERK inactivates the GAP and increases mTORC1 activity (Cully et al., 2010; Inoki et al., 2002; Ma et al., 2005). The mTORC1 plays a central role as an integrator of diverse growth-related cell signaling, strongly influenced by signals including mechanical, metabolic and oxidative stress, nutritional status, and growth factors (Miyazaki and Esser, 2009; Spangenburg, 2009).

HFC activates several mitogen-activated protein kinase (MAPK) pathways, which may contribute to hypertrophy through control of protein synthesis or satellite cell behavior. Activation of MAPKs may contribute to mTORC1 activation, but ERK and p38 MAPKs can also phosphorylate p70S6k on T421/S424 directly (Pullen and Thomas, 1997). MAPK-dependent activation of transcription factors including MEF2 and MyoD, separate from any effects on mTORC1, is necessary for myogenic differentiation of muscle precursor cells (Sabourin and Rudnicki, 2000; Wu et al., 2000). MAPKs are phosphorylated within a few minutes of several forms of mechanical stimulation, including active force generation and active or passive stretch (Hornberger et al., 2005; Martineau and Gardiner, 2001). ERK and p38 MAPK as well as p70S6k^{T389} phosphorylation are greater following heavy resistance exercise than light resistance, even at similar load×repetition levels (Holm et al., 2010), and phosphorylation of the MAPKs in general has been strongly correlated with force production (Martineau and Gardiner, 2001; Wretman et al., 2001).

Although mechanical loading is a potent signal, HFC consumes ATP and oxygen, imposing confounding metabolic stresses on the muscles. Notable among the metabolic sensors is AMP-activated

protein kinase (AMPK), primarily activated by the cellular AMP:ATP ratio. Metabolic stress and AMPK negatively influence cell size at least partly through inhibition of mTORC1 (Miyazaki and Esser, 2009; Spangenburg, 2009). AMPK knockout mice demonstrate elevated p70S6k T389 phosphorylation, protein synthesis and fiber size (Lantier et al., 2010). Artificial activation of AMPK by AICAR diminishes contraction-induced mTORC1 signaling, decreases protein synthesis and induces atrophy in myotubes and muscle (Bolster et al., 2002; Deshmukh et al., 2008; Thomson et al., 2008). However, in kinase-dead AMPKα2 mice, running induces exaggerated phosphorylation of ERK1/2 (Maarbjerg et al., 2009), and AICAR treatment activates p38 (Lemieux et al., 2003), indicating substantial interaction among AMPK and MAPK pathways. While AMPK signaling may be a key inhibitory modulator of cell growth through suppression of mTOR signaling under starvation conditions, its contribution to complex, contraction-induced stresses remains unclear.

The goal of this work is to distinguish between the mechanical and metabolic aspects of HFC. Force production cannot be decoupled from metabolic cost, but the relationship between force and metabolic cost is highly dependent on the conditions of stimulation. For example, concentric activation of muscle results in lower force production than isometric activation, but greater ATP consumption (Potma et al., 1994). Because force cannot be independently controlled, selecting a measure for the mechanical aspect is difficult. Ideally, such a measure would reflect only the mechanical stimulus, such as force, strain or work. However, signaling from a single contraction is difficult to resolve, and response magnitude accumulates during repeated contractions. This necessitates some kind of correction for repeated stimuli. Total work is a conceptually attractive measure, but work is zero during isometric activations. Force–time integral (FTI) is work-like, but imposes a false equivalency between high-load, low-repetition and low-load, high-repetition protocols. We have settled on FTI as a measure relevant in both mechanical and metabolic signaling, although the mechanical aspect is convoluted by the metabolic stress or contraction time aspect.

This study was designed to analyze phosphorylation state of kinases activated immediately following HFC under conditions emphasizing metabolic and mechanical stresses to test the hypothesis that high-frequency electrical stimulation (HFES) induces growth-related signaling proportional to mechanical stimulation. This hypothesis has been examined frequently (Garma et al., 2007; Hentzen et al., 2006; Martineau and Gardiner, 2001; Wretman et al., 2001), but past studies have relied heavily on eccentric activation to provide large mechanical stimuli, and eccentric activation uniquely induces an injury response, qualitatively different than isometric or concentric activation. In the present study, two experiments were performed, one emphasizing the metabolic aspect of HFC by manipulating the total time of activation (duty cycle) and the duration of stimulus trains, and one emphasizing the mechanical aspect by manipulating force magnitude while holding stimulation time constant. These interventions were intended to provide controlled changes in FTI under diverse mechanical and metabolic conditions, with the expectation that systematic FTI-dependent signaling would be observable across all conditions. That is, because it is not possible to design interventions in which only force is altered, these interventions were designed to vary as many force-influencing parameters as practical and to extract force signaling from the resulting data pool. Factor analysis was used to identify commonly correlated signaling modules within the mTOR and MAPK signaling networks. The results reveal a p38 MAPK–mTOR signaling module closely related to FTI, but separate from markers of metabolic load, and therefore linked to the mechanical aspect of HFC.

MATERIALS AND METHODS

Animals

Male CFW Swiss-Webster mice (Crl:CFW, Charles River, 26.2±2.0 g) were housed in pairs on a 12 h:12 h light:dark cycle with food and water provided *ad libitum*. In these animals, the tibialis anterior (TA) is a mixed fast oxidative/fast oxidative-glycolytic muscle, similar in composition to many hindlimb muscles (Burkholder et al., 1994). Procedures were reviewed and approved by the Institutional Animal Care and Use Committee at Georgia Institute of Technology and performed in compliance with the Guide for Care and Use of Laboratory Animals.

Electrical stimulation

Animals were anesthetized by intraperitoneal injection of a ketamine cocktail (90 mg kg^{-1} ketamine, 1 mg kg^{-1} acepromazine and 10 mg kg^{-1} xylazine). The TA muscle was surgically exposed, the distal tendon released and tied to the arm of a force-measuring servo motor (Aurora Scientific, Aurora, ON, Canada), and the knee immobilized in a spring clamp. The peroneal nerve was isolated and mounted on hook electrodes. A series of twitch activations was used to determine the current (I_0) and muscle length (L_0) producing maximal twitch force (P_t). Muscles were then subjected to a series of activations at 70 Hz, using one of the stimulation regimens described below. Throughout the stimulation protocol, muscles were wetted with 1× PBS (136.7 mmol l^{-1} NaCl, 2.7 mmol l^{-1} KCl, 1.4 mmol l^{-1} KH_2PO_4, 4.3 mmol l^{-1} Na_2HPO_4) or mineral oil to prevent desiccation. Immediately following electrical stimulation, animals were euthanized by cervical dislocation and the muscles were dissected and flash frozen in melting isopentane.

Metabolic load

To test the contribution of metabolic stress to HFC signaling, duty cycle (DC; the fraction of time during which the muscle was stimulated) and stimulation duration (StimDur; the duration of a single stimulus train) were chosen as the controlled variables. Therefore, the number of activations per group differs (Table 1). Thirty-two animals were randomly assigned to one of four experimental groups, with two independent factors: DC [low (LDC): 1.5% work:rest; high (HDC): 15%] and StimDur (short: 0.3 s; long: 3.0 s). HDC activations were performed as 10 sets of six or 60 activations with 1 min rest between each set, while LDC activations were evenly spaced over the 20 min protocol duration. In this protocol, FTI was expected to be most strongly influenced by total stimulation time, with smaller variation due to differences in fatigue, depending on the stimulation regimen.

Table 1. Stimulation parameters and force measures for low and high duty cycle protocols

Duty cycle	Low, 1.5%		High, 15%	
Stimulation duration	0.3 s	3 s	0.3 s	3 s
Rest (s)	20.3	240	0.85	10
Contraction number	60	6	600	60
FTI (N•s g^{-1})	0.50±0.1	0.27±0.1	2.27±0.9	2.34±0.7
Specific force (N cm^{-3})	2.90±0.5	2.93±0.4	2.85±0.6	3.07±0.3
Number of animals	9	13	13	14
Group	LDC-short	LDC-long	HDC-short	HDC-long

Means are presented ±s.d. FTI, force–time integral.

Force level

To test the contribution of force to HFC signaling, three target force levels were chosen with sub-maximal force levels achieved using three methods. In this protocol, FTI was expected to be most strongly influenced by force magnitude. The energetic cost of contraction and force have different correlations when force is manipulated through the force–length, force–velocity or force–stimulus intensity relationships, and this design was intended to decouple the metabolic and mechanical aspects of HFC. A total of 56 animals were randomly assigned to one of seven experimental groups. After determining L_0, maximal isometric tension (P_0) was determined by a 300 ms activation at 70 Hz. Muscles were then subjected to a series of 60 activations of 300 ms at 70 Hz, one train every 15 s, for a protocol duration of 15 min. Sub-maximal force was modulated by altering length (L), velocity (V) or pulse width (PW), as described below, to achieve moderate or low force levels: Mod-L, Mod-V, Mod-PW, Low-L, Low-V or Low-PW. Maximal tension (high) is produced during isometric activations at optimum length (L_0) and supramaximal pulse width, so High-L, High-V and High-PW groups represent identical conditions, and only one, lumped High group was used.

Length method

Short muscle lengths reduce the ability of the sarcomere to properly engage in cross-bridge formation and results in reduced force per fiber with a relatively constant metabolic load (Fenn and Latchford, 1933; Stephenson et al., 1989). After the single tetanus to determine P_0, muscles were shortened to reduce force generation. Based on force–length curves generated in a separate set of pilot experiments, Mod-L muscles were shortened by 2 mm, and Low-L muscles were shortened by 3 mm. These lengths were adjusted on subsequent stimuli to obtain active tensions of 60±10 or 30±10% of P_0 (Table 2).

Velocity method

Increasing shortening velocity reduces force by limiting cross-bridge efficiency, but increases cross-bridge turnover rate, resulting in a higher energetic cost (Huxley, 1957; Potma et al., 1994). After determination of P_0, target force was set and isotonic activations were performed using the muscle servo in force control mode. The Low-V force was 38.7% P_0, and Mod-V force was 68.7% P_0 (Table 2).

Pulse width method

Modifying the number of fibers activated results in force and metabolic load that are proportional to activation level. Preliminary force–pulse width curves were used to estimate the pulse width at which the target force would be produced. Force was monitored and pulse width periodically adjusted during the series of tetani to maintain target isometric force levels of 30±10 and 60±10% (Table 2). The current used for these stimulations was $1\times I_0$.

Force measurement

Muscle force during stimulation was digitized at 1000 Hz in 500 or 3500 ms windows surrounding each 300 or 3000 ms stimulation, respectively. The resting, passive tension was subtracted from each trace, and tension records were normalized to muscle mass. During concentric activations, length change and velocity were also recorded.

Several additional, derived measures of performance were calculated. Average peak force (APF) for each animal was determined by averaging the peak tension achieved across all six, 60 or 600 activations. FTI was determined by integrating force generated during all activations. Two measures of transient, contraction-induced force decline were defined. Sag is a measure of the force loss during a single activation and was defined as the difference between force at the end of each activation and the peak force achieved during that activation, normalized to the peak force, and averaged across all activations. Fatigue was defined as the difference in peak force between the most forceful activation and the final activation.

The time constants associated with force decline within individual activations were determined by fitting the force decline during

Table 2. Stimulation protocol and characteristics of muscles producing two sub-maximal force levels (moderate and low) by three methods (length, velocity and pulse width) that will be compared with the high force level

Method	Parameters	High force (100% P_0)	Moderate force (60% P_0)	Low force (30% P_0)
Length	Average peak force	–	57.9±7.4% (14.0 N g^{-1})	30.7±3.7% (7.3 N g^{-1})
	Intra-animal variability		3.1±3.0%	6.9±4.7%
	Force–time integral		0.24±0.04 N•s g^{-1}	0.09±0.03 N•s g^{-1}
	Specific force		2.8±0.2 N cm^{-2}	2.5±0.2 N cm^{-2}
	Mode		Isometric	Isometric
	Length		−1.84±0.52 mm	−2.54±0.51 mm
Velocity	Average peak force	–	68.7±0.8% (14.8 N g^{-1})	38.6±1.1% (8.3 N g^{-1})
	Intra-animal variability		1.1±2.8%	0.17±0.1%
	Force–time integral		0.31±0.03 N•s g^{-1}	0.18±0.03 N•s g^{-1}
	Specific force		2.8±0.1 N cm^{-2}	2.8±0.5 N cm^{-2}
	Mode		Concentric	Concentric
	Length change		−0.8±0.3 mm	−2.1±0.2 mm
	Peak velocity		6.1±1.4 mm s^{-1}	16.0±1.5 mm s^{-1}
Pulse width	Average peak force	–	62.9±6.0% (12.7 N g^{-1})	29.3±3.8% (6.6 N g^{-1})
	Intra-animal variability		7.1±1.8%	10.0±2.4%
	Force–time integral		0.23±0.06 N•s g^{-1}	0.14±0.03 N•s g^{-1}
	Specific force		2.6±0.5 N cm^{-2}	2.9±0.2 N cm^{-2}
	Mode		Isometric at L_0	Isometric at L_0
	Pulse width		~0.06 ms	~0.03 ms
All	Max force (P_0)	24.2±4.9 N g^{-1}	–	–
	Force–time integral	0.46±0.09 N•s g^{-1}		
	Specific force	3.1±0.6 N cm^{-2}		

Data are means ± s.d.

tetanus to a sum of two exponentials. For HDC-short, the rate of decline in peak force between successive activations was also analyzed.

Western blotting

For protein analysis, frozen muscles were transected at the midline, and the proximal half was homogenized using a rotor-stator (TissueMizer, Fisher Scientific, Pittsburgh, PA, USA) in a low salt detergent buffer (50 mmol l^{-1} Tris, pH 7.5; 30 mmol l^{-1} NaCl; 5 mmol l^{-1} EDTA, 1% Triton X-100 plus 100 mmol l^{-1} NaF, 1 mmol l^{-1} $NaVO_3$ and protease inhibitors) to minimize myofilament extraction and cleared of debris at 15,000 ***g***. The protein concentration of the supernatant was measured by bicinchoninic acid assay (Pierce, Rockford, IL, USA) according to the manufacturer's protocol.

Soluble protein (15 μg) was separated by SDS-PAGE, transferred to nitrocellulose membranes and detected by western blot. Stimulated and contralateral muscles from the same animal were always loaded in adjacent lanes, but the arrangement of animals across gels was randomized. Each gel and blot was performed at least twice, and the average outcome was used for analysis. Primary antibody dilutions were: p-ERK$^{T202/T204}$ 1:3000; total ERK2 1:2500; p-JNK 1:500; p-p38$^{T180/Y182}$ 1:2000; p-Akt^{S473} 1:2000; total Akt 1:2000; p-P70S6k$^{T421/S424}$ 1:2000; p-p70S6k^{T389} 1:2500; pan p70 1:2000; p-ACC 1:1000; p-mTORC1^{S2448} 1:2000; and p-FAK^{Y397} 1:2000. All antibodies were purchased from Cell Signaling (Danvers, MA, USA) except JNK (Santa Cruz Biotechnology, Santa Cruz, CA, USA), FAK (Invitrogen, Carlsbad, CA, USA) and total ERK2 (BD, San Jose, CA, USA). Bands were visualized by enhanced chemiluminescence and quantified by scanning densitometry. Results are expressed as a ratio of the stimulated to the unstimulated contralateral muscle. P-JNK, p-p38, p-mTOR and p-FAK are expressed as IOD_{stim}/IOD_{unstim}, where IOD is the integrated optical density of the band, and stim/unstim refers to the stimulated muscles and unstimulated, contralateral muscles, respectively. p-ERK, p-Akt and p-p70S6k are expressed as $(IOD_{stim}/IOD_{unstim})/(IOD_{stim\text{-}pan}/IOD_{unstim\text{-}pan})$, where pan refers to the corresponding non-phosphorylated, or total, antigen. Acetyl-CoA carboxylase (ACC) phosphorylation was quantified by normalizing all of the bands on a gel to the average of the contralateral IOD from all animals on that gel. Each blot included a common positive control from insulin stimulated or eccentrically activated TA muscle for validation.

Glycogen content

The distal portion of the TA was weighed and digested in 30% KOH saturated with Na_2SO_4 for 20 min at 100°C. Glycogen was precipitated with 1.2 volumes of 95% EtOH for 30 min on ice as described by Lo (Lo et al., 1970), pelleted at 850 ***g*** for 30 min, and dissolved in deionized H_2O. Glycogen content was determined spectrophotometrically using 5% phenol followed by rapid addition of 96% H_2SO_4 and read at 490 nm.

Statistics

All values are expressed as means ± s.d. and statistical analyses were performed in StatView (SAS Institute, Cary, NC, USA). Glycogen content was analyzed by three-way, mixed model, repeated-measures ANOVA, with stimulated/contralateral as a repeated measure and DC and StimDur as factors. Western blot ratios (stimulated:contralateral) were log transformed for statistical analysis, although untransformed results are presented in tables and graphs. Phosphorylation ratios were subjected to one-sample *t*-tests to determine whether electrical stimulation caused any change in phosphorylation relative to contralateral (100%, by definition). Differences among treatments were then identified by two-way ANCOVA (StimDur × FTI or method × FTI) with a significance threshold of $P<0.05$, followed by *post hoc* *t*-tests using the Bonferroni–Dunn correction for multiple comparisons. Because the one high force group is common to all stimulation methods and the software requires a fully populated data matrix, the high force data were replicated and represented in all methods. Replication of data increases the degrees of freedom used for statistical analysis and results in an overestimate of significance. To account for this, *F*-values were recalculated using corrected degrees of freedom and *P*-values were recalculated using the F to P calculator at http://vassarstats.net/tabs.html.

Because of the breadth of data obtained from each sample, factor analysis was used to extract principal components and identify potential common causes. Kinase ratios, FTI, glycogen content and fatigue were included in this analysis with the anticipation that common causes within a group of kinases might allow resolution of more subtle mechanical effects than individual kinases. Factor scores were varimax transformed and method-dependent differences in the orthogonal solutions were determined by ANOVA with a significance threshold of $P<0.05$.

RESULTS

This study used two different strategies to manipulate FTI: one emphasizing the metabolic aspect of FTI by changing stimulation duty cycle, and one emphasizing the mechanical aspect of FTI by changing activation conditions. Results of the duty cycle experiments are reported first.

Force variation during high duty cycle activations

Within the DC/StimDur protocols, peak force produced during the first activation was 1.12±0.2 N or 22.9±3.5 N g^{-1} and did not differ between groups. However, the force profiles were substantially different among protocols (Fig. 1), characterized by failure to maintain tension during an activation or sag, especially in the long contraction groups, and fatigue in the HDC groups (Fig. 1, inset). Sag was not different between long activations, averaging 60±16 and 62±22% in HDC-long and LDC-long, respectively. In LDC-short, sag averaged 5.4±8%, and 27±17% in HDC-short. In the HDC groups, where activations were grouped into sets, there was a decline in peak force between activations within a set and substantial recovery of peak force during the extended inter-set rest period. This fatigue–recovery process was most dramatic in HDC-short, in which force decline from the first activation of a set to the second was as high as 50%. Fatigue was greatest in the HDC-short program, 60.6±8%, compared with 20.6±11% in HDC-long (Fig. 2A). In contrast, during LDC-short, force increased by 13% from 22.5±3.7 to 25.5±3.2 N g^{-1}, and two-way ANOVA revealed a significant interaction between DC and StimDur ($P<0.0001$; Fig. 2A).

FTI was greater in the HDC protocols ($P<0.0001$; Table 1, Fig. 2B) because of the greater total time of stimulation. In the LDC regimen, sag during long activations reduced FTI relative to short stimulations (LDC-long: 0.27±0.1 N s g^{-1}, LDC-short: 0.50±0.1 N s g^{-1}). At high duty cycle, force reduction due to fatigue in HDC-short balanced the force decline due to sag in HDC-long, and resulted in very similar FTI (HDC-long: 2.34±0.7 N s g^{-1}, HDC-short: 2.27±0.9 N s g^{-1}; Fig. 2B, Table 1).

FTI-dependent metabolic load

Regression analysis revealed the expected correlations between FTI and ACC phosphorylation ($R=0.606$, $P<0.0001$) and glycogen

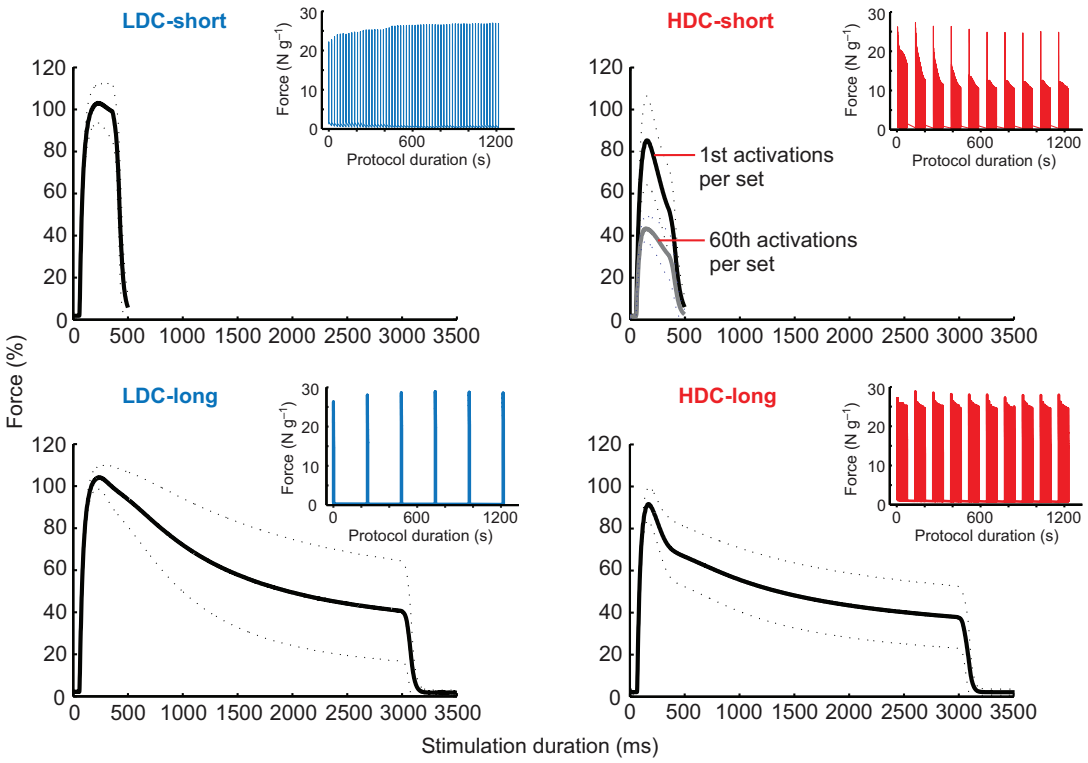

Fig. 1. Average forces produced by the four metabolic stimulation protocols as labeled. Solid lines represent the mean of all traces, and dotted lines represent ±s.d. for each animal. Long duration activations result in substantial sag, or loss of tension, during an activation. Because of the dramatic fatigue, or loss of tension between successive activations, in HDC-short, the black trace represents the average of the first activations from each of 10 sets and the gray trace represents the average of the 60th activations from each of 10 sets. Insets are representative muscle force traces for each complete protocol and show the differences in fatigue.

content (R=0.397, P=0.007). The greater metabolic load imposed by HDC protocols was associated with greater ACC phosphorylation (P=0.0012), but no effect of stimulation duration nor their interaction could be resolved (Fig. 2C). Analysis by three-way, mixed model ANOVA confirms that glycogen content was reduced in muscles following electrical stimulation (main effect of stimulation, P=0.016, Fig. 2D), dependent on duty cycle (stimulation × DC interaction, P=0.032). Glycogen content was weakly correlated with fatigue (R=0.340, P=0.02), but the dramatic fatigue in HDC-short was not associated with exaggerated glycogen depletion or ACC phosphorylation.

Metabolic FTI-dependent phosphorylation of signaling molecules

Phosphorylation of each antigen was expressed as a fraction of contralateral is given in Table 3, and representative western blots are shown in Fig. 3A. One-sample t-tests revealed that electrical stimulation resulted in changes in phosphorylation of all three MAPKs (p38, P<0.0001; ERK2, P<0.0001; p54 JNK, P<0.0001), Akt (P<0.0001), mTOR (P=0.003) and p70S6k on T421/S424 (P<0.0001), but not on T389 (P=0.61) or FAK (P=0.06). To understand the relative role of FTI and StimDur in these changes, results were further analyzed by ANCOVA, which did not resolve any systematic effect of FTI or StimDur on ERK, JNK or Akt. A systematic effect of FTI (Fig. 3B) was found only for p38 (P=0.0009) and mTOR (P=0.003), and a trend for p70S6k on T421/S424 (P=0.080). A weak interaction between FTI and StimDur was found in ERK2 (P=0.046), with phosphorylation tending to increase with DC during long activations, but to decrease with DC during short activations. Despite the dramatic fatigue in HDC-short, only phosphorylation of p54 JNK was significantly correlated with fatigue (P=0.035; Fig. 3C).

Systems analysis

To clarify relationships among the many variables, data were further analyzed by factor analysis to identify statistically correlated sets of variables or signaling modules (Fig. 4). Factor analysis identifies groups of parameters that covary, and ANOVA of the resulting factor scores may reveal a coherent response to the experimental design stimuli. Five factors were identified, accounting for 100% of the population variance. The contribution of individual measures to those five factors is shown in Fig. 4A, with contributors greater than 0.4 highlighted.

The extracted factors reinforce the interpretation of individual data, identifying signaling modules separately associated with FTI and fatigue. Factor 2 has high weightings for FTI (0.568) and p-ACC (0.679) and includes p-mTOR (0.894) and p-p38 (0.418), consistent with the ANCOVA (Fig. 3B). Likewise, Factor 4 has a high weighting for fatigue (0.457), coupled with p54 JNK (0.904) phosphorylation. Factor 5 combines both force measures (FTI: −0.649, fatigue: 0.678) and glycogen content (0.822), and is the only factor to show significant interaction between StimDur and DC (P=0.049; Fig. 4A).

Distinct force levels produced with low metabolic cost

The results above closely link phosphorylation of mTOR and p38 with FTI and ACC phosphorylation, supporting equally a mechanical or metabolic stimulus. To separate the force and metabolic aspects

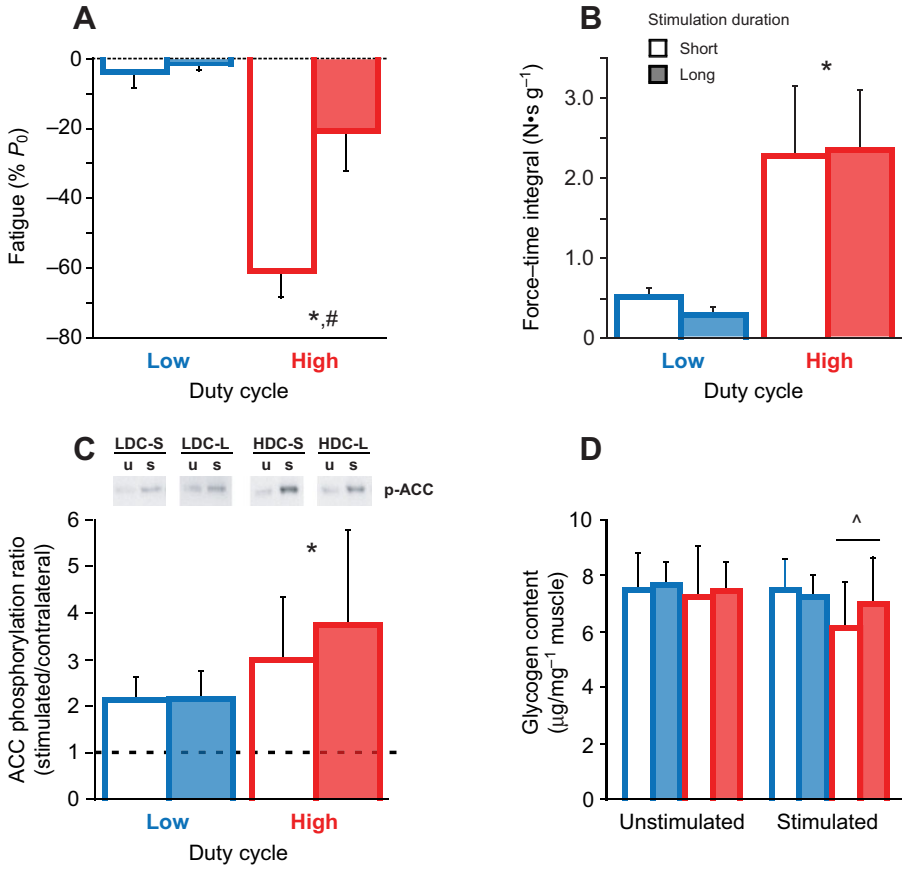

Fig. 2. Summary statistics for (A) fatigue, (B) force–time integral (FTI), (C) ACC phosphorylation and (D) glycogen content of low (LDC, blue) and high (HDC, red) duty cycle activations of short (open bar) and long (filled bar) duration. (C) Representative western blots for ACC phosphorylation of unstimulated (u) and stimulated (s) muscles are shown from a single gel. (D) Glycogen content is shown for both stimulated muscles and unstimulated, contralateral muscles. Data are means ± s.d. In A–C, * indicates a significant effect of DC, and # a significant effect of stimulation duration (StimDur) by two-way ANOVA. In D, ^ indicates a significant interaction between stimulation and duty cycle by three-way ANOVA.

of this signaling module, contractions were produced under conditions that minimize the metabolic stress (i.e. a low duty cycle protocol using short duration activations) while producing a range of FTIs.

Forces produced during the seven force–method protocols are shown in Fig. 5A and detailed in Table 2. Across methods, the APF of all 60 activations was 99.5±6.9% for high, 64.8±5.3% for moderate and 35.2±5.8% of P_0 for low force groups. Peak force is maintained during successive activations (Fig. 5B), and the APF produced is highly correlated with FTI (R=0.895, P<0.0001). Conserved force production is also reflected in low ACC phosphorylation, increased by only 40±25% (one-sample t-test, N=56, P<0.0001) over contralateral, with no systematic variation among groups (method, P=0.52; FTI, P=0.09). Likewise, no systematic effect of stimulation on glycogen content could be resolved by ANCOVA (method, P=0.25; FTI, P=0.39; method × FTI, P=0.46).

Mechanical FTI-dependent phosphorylation of signaling molecules

Phosphorylation of each antigen, expressed as a fraction of contralateral, is given in Table 4, with representative western blots in Figs 6 and 7. Positive control samples (insulin or eccentric activation) were included on each blot to validate antigen detection and sensitivity (Fig. 6). Similar to the DC/StimDur experiment, one sample t-tests confirmed that electrical stimulation induced changes in all three MAPKs (p38, P=0.0006; ERK2, P<0.0001; p54 JNK,

Table 3. Group phosphorylation (fraction of contralateral), glycogen content (fraction of contralateral) and force results (means ± s.d.) from the DC/StimDur stimulations

Measure	LDC-short	LDC-long	HDC-short	HDC-long	FTI P-value
p38	4.04±2.27	3.28±2.01	7.68±4.71	5.87±3.23	**0.001**
JNK46	1.12±0.24	1.14±0.64	1.01±0.38	1.25±0.30	0.756
JNK54	4.90±4.05	6.15±3.58	3.82±1.45	5.59±2.61	0.931
ERK2	6.03±2.75	7.05±6.83	5.38±2.89	9.74±5.95	0.931
AKT	0.55±0.22	0.46±0.11	0.66±0.27	0.56±0.31	0.271
mTOR	1.08±0.30	1.13±0.38	1.35±0.43	1.51±0.70	**0.003**
p70-421	2.46±1.24	2.29±1.29	2.82±1.27	2.83±1.48	0.080
p70-389	0.93±0.30	1.15±0.53	1.13±0.52	1.14±0.58	0.643
FAK	0.97±0.25	1.14±0.42	1.16±0.42	1.46±0.88	0.209
ACC	2.11±0.47	2.11±0.60	3.19±1.35	3.79±2.09	**<0.001**
Glycogen	1.01±0.09	1.01±0.56	0.86±0.17	0.93±0.16	**0.006**
APF (%)	109±10	109±13	54±7	95±9	
FTI (N•ms g^{-1})	0.50±0.10	0.27±0.09	2.42±0.86	2.32±0.76	

FTI P-value indicates the P-value for the main effect of FTI in StimDur × FTI ANCOVA.

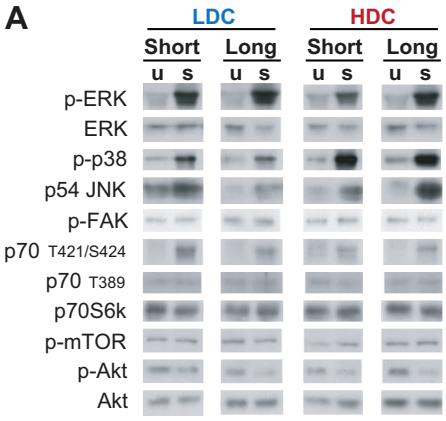

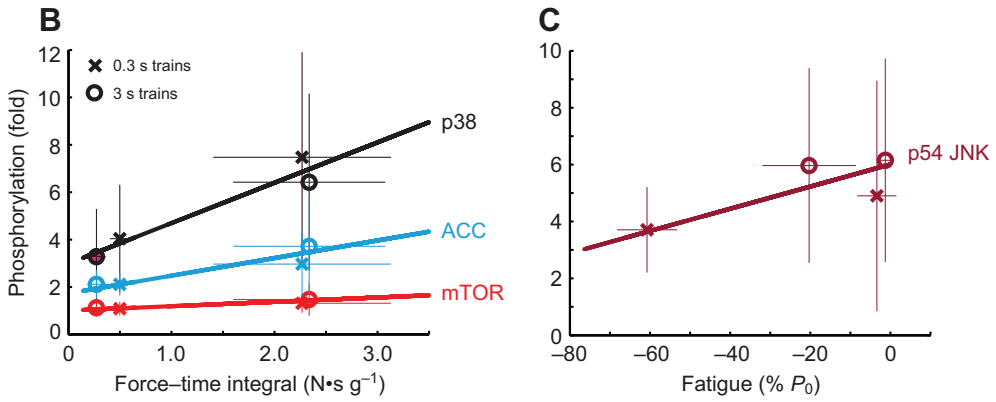

Fig. 3. (A) Representative western blots for contralateral, unstimulated muscles (u) and stimulated muscles (s). All blots shown for a single protein are generated from a set of muscles analyzed together on the same gel, but not in the order presented. (B) Regression plots of phosphorylation of p38, ACC and mTOR against FTI. (C) Phosphorylation of p54 JNK correlated with fatigue. Regression was performed against individual data points, but protocol averages are shown for clarity. Bars represent ±s.d. in each axis.

$P<0.0001$), Akt ($P<0.0001$) and p70S6k on T421/S424 ($P<0.0001$), but not on T389 ($P=0.46$) or FAK ($P=0.71$). ANCOVA again failed to resolve many systematic effects of FTI or method. A significant main effect of FTI could only be resolved in $p70S6k^{T421/S424}$ (Table 3, $P=0.037$) and FAK ($P=0.008$). Regression of FAK phosphorylation against FTI (Fig. 7A) illustrates the consistent relationship between the mechanical input and the signaling output, independent of the method of modulating the mechanical input that should characterize mechanical signaling. A significant main effect was found for method on phosphorylation of ERK2 ($P=0.012$) and a trend on $p70S6k^{T421/S424}$ ($P=0.07$). In both cases, the pulse width group, in which force was decreased by de-recruiting motor units, is lower than the other methods, suggesting that phosphorylation of those molecules may occur specifically in stimulated fibers.

The lack of main effects in p38 appeared to result from exaggerated phosphorylation in a single low force point in the velocity method (Fig. 7B). Analysis without this outlier uncovered a main effect of FTI ($P=0.04$, Fig. 7B). In neither analysis did an interaction effect appear (method × FTI, $P=0.19$ including or $P=0.63$ excluding outlier). Detailed examination of the outlying data point, including repeated western blots, failed to uncover any justification for excluding it beyond being vastly different than all other samples, but further analysis excludes this point. With exclusion, the regression lines (Fig. 7B) in the length and pulse width methods are nearly identical, and the slope difference in the velocity method could not be statistically resolved ($P=0.19$). Thus, p38 is the most directly force-dependent MAP kinase in this study.

One exception to the equivalence between FTI and APF as force measures was found in phosphorylation of ERK2. Although there was no interaction between FTI and method, the interaction between APF and method is significant ($P=0.028$; Fig. 7C). Under the pulse width method, ERK2 phosphorylation was positively correlated with APF ($P=0.036$). However, under the length method, ERK2 phosphorylation was negatively correlated with APF ($P=0.046$), and no correlation was found under velocity modulation ($P=0.92$). The discrepancy between APF and FTI results from more apparent sag in the length method, resulting in a method-dependent decoupling of FTI and APF, with length-APF being systematically larger than length-FTI. In the APF ANCOVA, this shifts the low-force length points to larger numbers, increasing the apparent slope of the relationship, and reaching the threshold for significance.

Mechanical systems analysis

In the force–method data set, factor analysis extracted three factors (Fig. 8A) accounting for 83% of the population variance. Mechanical Factor 2 is similar to Metabolic Factor 2, containing FTI (0.426), p38 (0.715) and mTOR (0.715), but increasing FAK (0.608 *vs* 0.252) and reducing ACC (0.308 *vs* 0.679). It is worth noting that, although mTOR and FAK are major signaling components of this factor, their phosphorylation, relative to contralateral muscles, could not be resolved. FTI is also a component of the Mechanical Factor 3 (−0.692), along with ACC phosphorylation (0.763), but with little contribution from any signaling molecule, similar to Metabolic Factor 5. ANCOVA of the resulting factor scores revealed that Factors 2 and 3 show strong, but opposite correlations with FTI. The relationships between the primary components of Factor 2 (p38) and 3 (ACC) with FTI confirm the opposite correlations with FTI (Fig. 8B). Together, these data indicate the signaling molecules associated with Mechanical Factor 2 are decoupled from the metabolic signaling associated with FTI in Mechanical Factor 3.

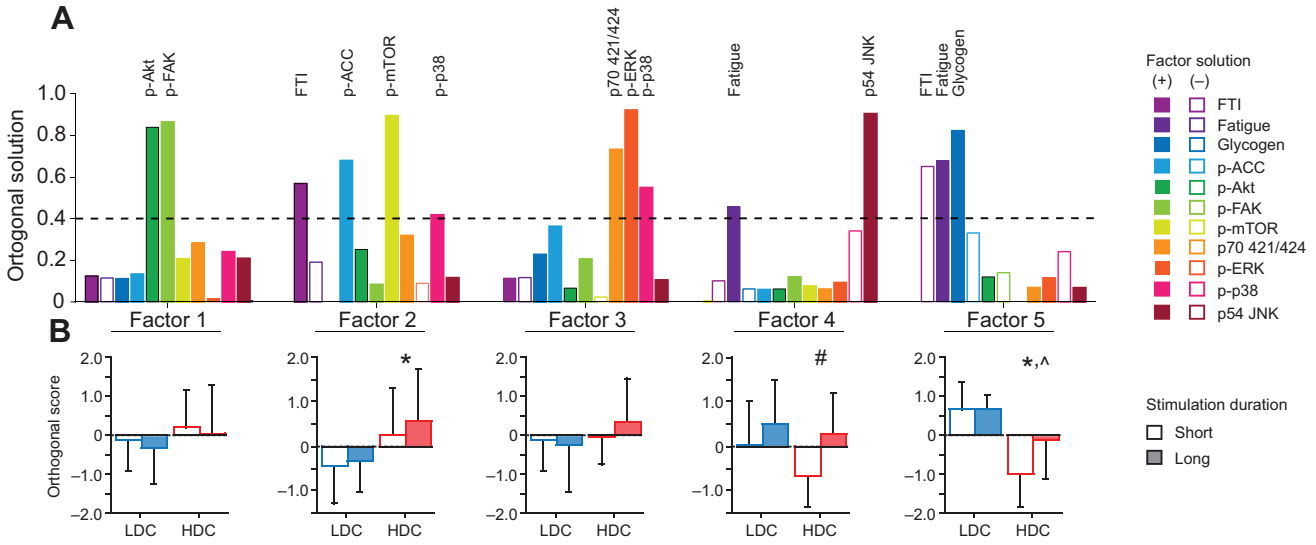

Fig. 4. (A) Component contributions of factors identified by factor analysis of the DC/StimDur data. Bars with a positive (filled) or negative (open) loading greater than 0.4 indicate primary components of that factor. (B) Two-way ANOVA of factor scores separated by LDC (blue) and HDC (red) with short (open bar) and long (filled bar) stimulation duration for each factor (means ± s.d.). * indicates significant main effect of DC, # indicates a main effect of StimDur and ^ indicates a significant interaction of DC × StimDur.

DISCUSSION

Principal findings

HFES induced strong phosphorylation of ERK, p38, JNK and p70S6k$^{T421/S424}$, with phosphorylation of p38, mTOR and ACC correlated with FTI. Under minimal metabolic load, the correlation between p38 phosphorylation and FTI persisted, although neither phosphorylation of ACC nor glycogen depletion could be resolved. Factor analysis indicated that the FTI–p38 module includes mTOR in both models, but the weighting of ACC is substantially reduced under low metabolic load. Persistence of the relationship among FTI, p38 and mTOR across both stimulation paradigms suggests that they form a coherent signaling module sensitive to the mechanical aspect of FTI.

Duty cycle alters metabolic stress

Metabolic stress is used in this work as a broad term encompassing the acute depletion of ATP and increased glycolytic and mitochondrial flux required to restore ATP. In this general sense, the magnitude of metabolic stress can be inferred from both biochemical and functional measurements. Biochemical measures

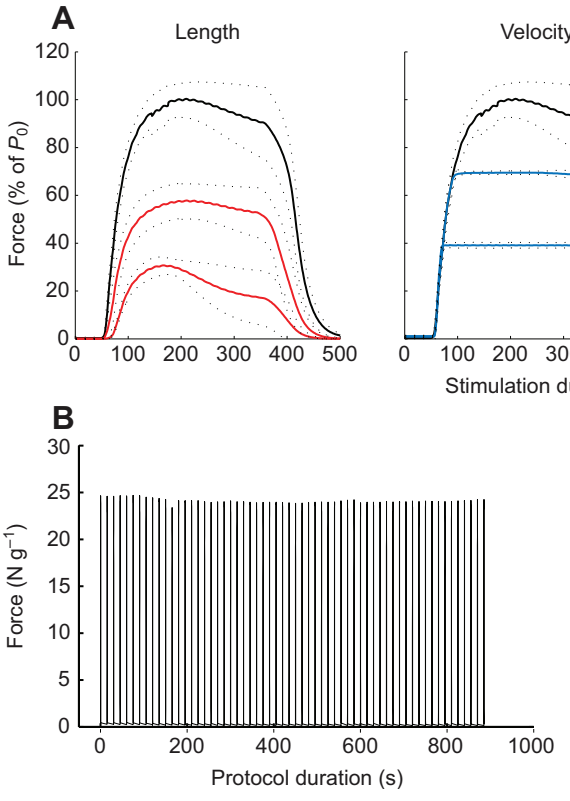

Fig. 5. (A) Forces produced by each group were first averaged across all 60 activations for each muscle, then averaged across all animals per group (*N*=8). Dashed lines represent ± s.d, and the high force data (black lines) are repeated across all three methods. (B) Representative force history for a single high force animal to show the conservation of force with repeated stimulation.

Table 4. Group phosphorylation (fraction of contralateral), glycogen content (fraction of contralateral) and force results (means ± s.d.) from the force–method stimulations

Measure	High	LT60	LT30	FV60	FV30	PW60	PW30	FTI *P*-value
p38	1.60±0.68	1.38±0.54	1.05±0.39	1.62±0.96	1.49±0.29 2.64±3.27†	1.09±0.26	1.14±0.60	**0.039**
JNK46	1.01±0.43	1.01±0.14	0.83±0.16	1.06±0.46	1.23±0.45	0.91±0.23	1.05±0.44	0.86
JNK54	3.14±1.35	2.71±1.50	2.94±1.70	4.10±2.45	3.68±1.75	4.16±2.49	3.59±1.89	0.35
ERK2	5.47±3.71	5.56±3.20	8.69±5.56	7.60±3.04	4.58±1.61	4.25±2.32	2.43±0.88	0.11
AKT	0.62±0.29	0.58±0.23	0.81±0.59	0.84±0.23	0.78±0.36	0.51±0.11	0.60±0.36	0.84
mTOR	1.14±0.54	1.10±0.39	0.97±0.36	0.92±0.24	1.04±0.23	0.95±0.44	1.10±0.41	0.59
p70-421	1.94±0.53	2.02±0.98	5.55±4.84	3.83±1.27	3.04±1.08	2.21±0.99	2.10±1.32	0.29
p70-389	1.01±0.44	0.96±0.53	1.20±0.47	1.04±0.56	1.13±0.33	1.19±0.38	1.16±0.26	0.85
FAK	1.89±1.21	1.33±0.41	1.14±0.44	1.29±0.69	1.84±1.81	1.05±0.33	1.13±0.42	**0.008**
ACC	1.16±0.41	2.12±0.58	1.55±0.78	1.32±0.30	1.65±0.62	1.24±0.53	1.40±0.58	0.09
Glycogen	0.93±0.21	0.86±0.12	0.89±0.19	0.97±0.15	0.97±0.18	0.94±0.13	0.93±0.13	0.89
APF (%)	106±13	72±12	38±8.5	64±13	31±4.6	73±4.0	42±4.1	
FTI (N•ms g^{-1})	0.46±0.09	0.24±0.04	0.09±0.03	0.31±0.03	0.18±0.03	0.23±0.06	0.14±0.03	

FTI *P*-value indicates the *P*-value for the main effect of FTI in method × FTI ANCOVA.
†p38 phosphorylation ratio including the outlying point indicated in Fig. 7.

of glycogen content and ACC phosphorylation indicate that HDC imposes a higher metabolic load than LDC, but failed to resolve any influence of force magnitude during low duty cycle stimulations. The recovery heat following a single activation is much less than the response to multiple stimuli (Barclay et al., 1995), indicating the activation of more extensive energy recovery processes by repeated stimulation, particularly at duty cycles in excess of 4%. We interpret duty cycle as primarily a metabolic stimulus, dependent on substrate depletion, and oriented at restoring the energy balance. High duty cycles are common among studies of HFC-induced signaling, and groups using protocols similar to HDC-long also report increased ACC phosphorylation (Thomson et al., 2008) and reduced glycogen content (Nader and Esser, 2001; Russ, 2008), although the reduction in glycogen appears to be greater in rats (Nader and Esser, 2001) than in mice (present study).

Force measurements also indicate that HDC imposes higher metabolic load. Barclay and co-workers (Barclay et al., 1995) found a very close correlation between heat production during an activation and decline in peak force of a second activation, indicating that decline in peak force is a useful proxy for energy expenditure. During LDC activations, peak force was maintained throughout both protocols, suggesting that ATP and phosphocreatine stores are sufficient for 300 ms activations, and that 20 s rest between activations is sufficient to restore high-energy phosphate balance. During HDC activations force declines during individual trains, and the pattern of fatigue between successive trains differed with StimDur and the rest period between activations. A small, consistent decline in force was observed within HDC-long sets, where a rest of 10 s separates successive activations, and this fatigue recovers almost completely during the 60 s rest between sets. This is consistent with Challiss and co-workers' observation that phosphocreatine is depleted by 50% during a single 3 s stimulation, recovers by 33% after 10 s rest, and recovers by 75% after 60 s (Challiss et al., 1989). By contrast, the fatigue observed within HDC-short sets, where less than 1 s separated successive activation, is

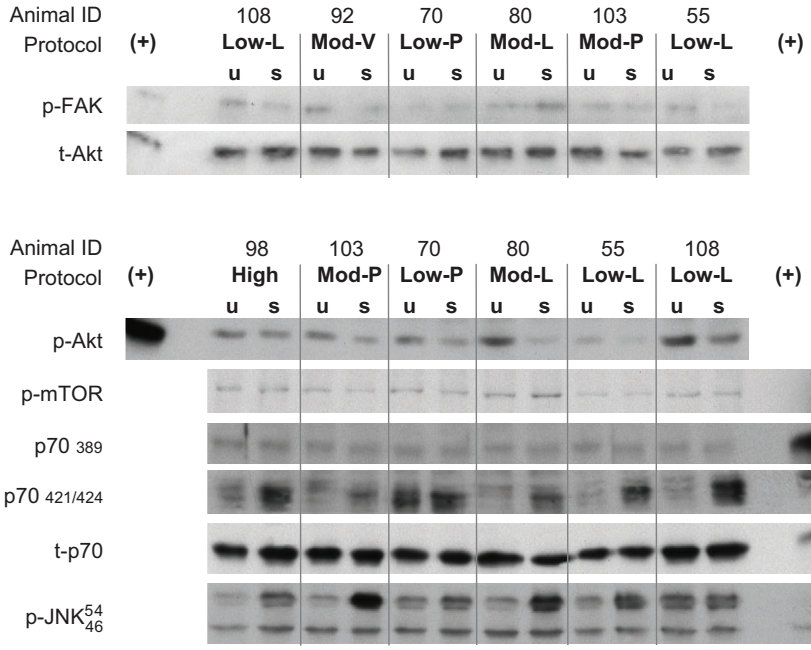

Fig. 6. Representative western blots for contralateral, unstimulated muscles (u) and stimulated muscles (s). All blots shown are generated from a single set of muscles analyzed together on the same gel with positive controls from either insulin-stimulated or eccentric-activated control muscles. Data are quantified in Table 3.

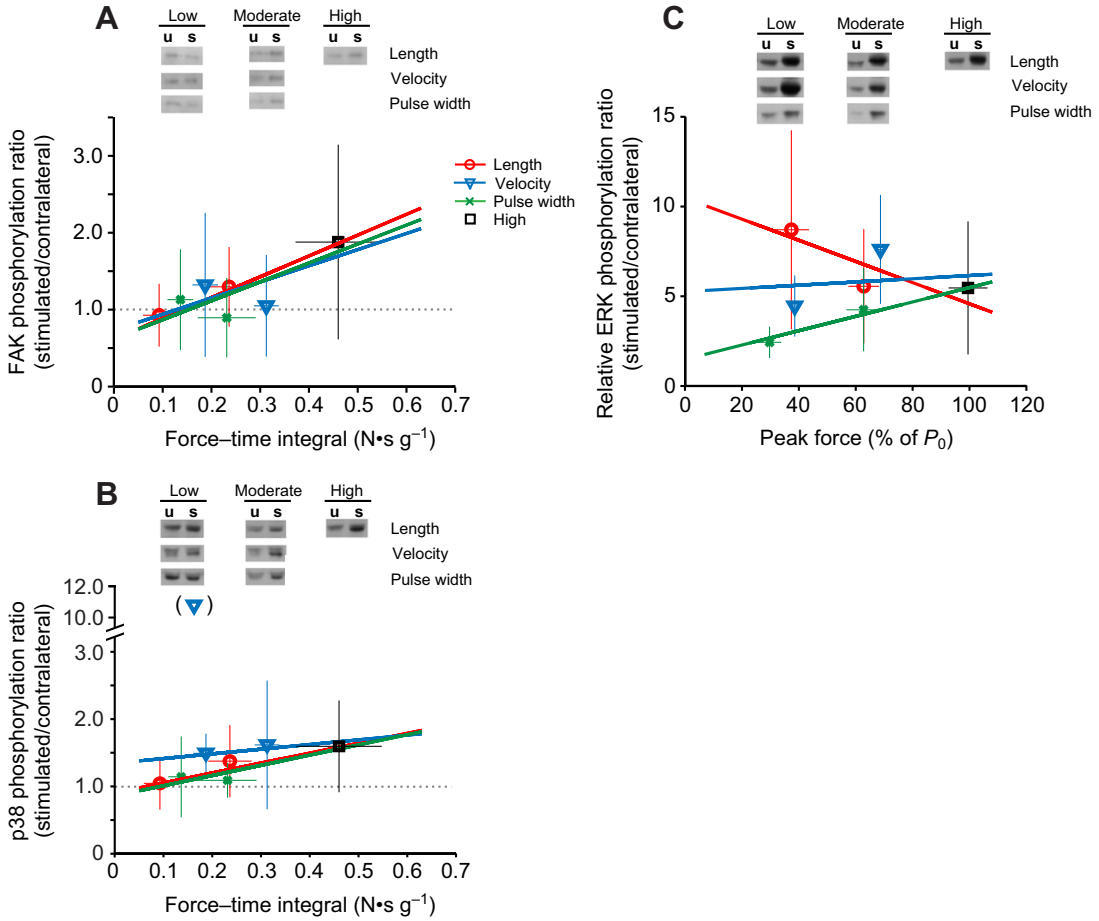

Fig. 7. Regression analysis of phosphorylation ratios (stimulated/contralateral) for FAK (A), p38 (B) and ERK (C) against the mean force–time integral (FAK, p38) or average peak force (ERK) in the force–method experiment. Regression lines were determined from individual data points, but group means (±s.d.) are plotted for clarity. Data are identified by method: length (red, circles), velocity (blue, triangles) and pulse width (green, ×). The high force group is represented by black squares. Representative western blots for contralateral, unstimulated muscles (u) and stimulated muscles (s) for each method and force level are shown above, in which blots from each method are from a single gel, arranged by pairs for readability.

much greater, suggesting that metabolite depletion can not be recovered during 1 s rest. So, duty cycle over an extended exercise bout appears to be a more potent metabolic stimulus than the duration of a single activation.

Mechanical activation of a p38–mTOR axis

A p38–mTOR signaling module was identified in both the metabolic stress (DC/StimDur) and force–method experiments. Under HDC activations, the p38–mTOR module positively correlates with ACC phosphorylation and FTI, which highlights the difficulty in separating mechanical and metabolic signaling, as one major measure of mechanical signaling, FTI, covaries strongly with a major measure of metabolic signaling (see Fig. 4). The objective of the force–method stimulations was to minimize the metabolic stimulus, but the p38–mTOR module remains correlated with FTI (Fig. 8, Factor 2) suggesting p38 phosphorylation is more responsive to FTI than metabolic load.

In the force–method experiments, even though metabolic load was below statistical resolution, the methods for manipulating force were chosen to decouple mechanical and metabolic signaling. This is most apparent when comparing between the pulse width and velocity measures. Under the pulse width method, where force was reduced by de-recruiting fibers, metabolic cost should be positively correlated with force and FTI. In contrast, accelerated crossbridge turnover during shortening increases ATP hydrolysis and heat production (Potma et al., 1994), and one would expect metabolic stress to be negatively correlated with FTI. So, where the number of repetitions was constant, correlations between force or FTI and signaling responses should be the same for mechanical signaling, as is seen in FAK phosphorylation (Fig. 7A), and reversed for metabolic signaling, as is seen in ERK phosphorylation (Fig. 7C). If p38 signaling were derived from an indirect metabolic stimulus, then it would be negatively correlated with FTI in the velocity method and positively correlated with FTI in the pulse width method, but two-way ANCOVA could not resolve a difference between these groups (Fig. 7B). The positive correlation between p38 and FTI was smaller (slope=0.14) using the velocity method than it was under the pulse width (slope=0.43) or length methods, but it was still positive.

The results of the force–method experiments identify p38 and FAK as molecules phosphorylated in a force-dependent manner. This is consistent with the widely recognized role of FAK and other members of the integrin-associated focal adhesion complex as mechanotransducers (Flück et al., 1999; Lal et al., 2007). Phosphorylation of p38 increased in response to HFC-induced mechanical stress (Nader and Esser, 2001; Wretman et al., 2001) or passive mechanical stretch (Aikawa et al., 2002). The correlations between FTI, FAK and p38 may represent a single pathway, as a hypertrophic signaling pathway involving integrin-FAK and p38 induced by mechanical stress has been reported (Aikawa et al., 2002; Lal et al., 2007). Activation of p38 may contribute to increased protein synthesis *via* phosphorylation of TSC2- and MNK-induced phosphorylation of eIF4E and p70S6k on T421/S424 (Cully et al., 2010; Hernández et al., 2011; Wang et al., 1998) and is required for myogenic differentiation *via* activation of MEF2 and MRF4 (Lluís et al., 2006), both processes required for muscle hypertrophy. The correlation found between p38 and mTOR in both experiments is consistent with the

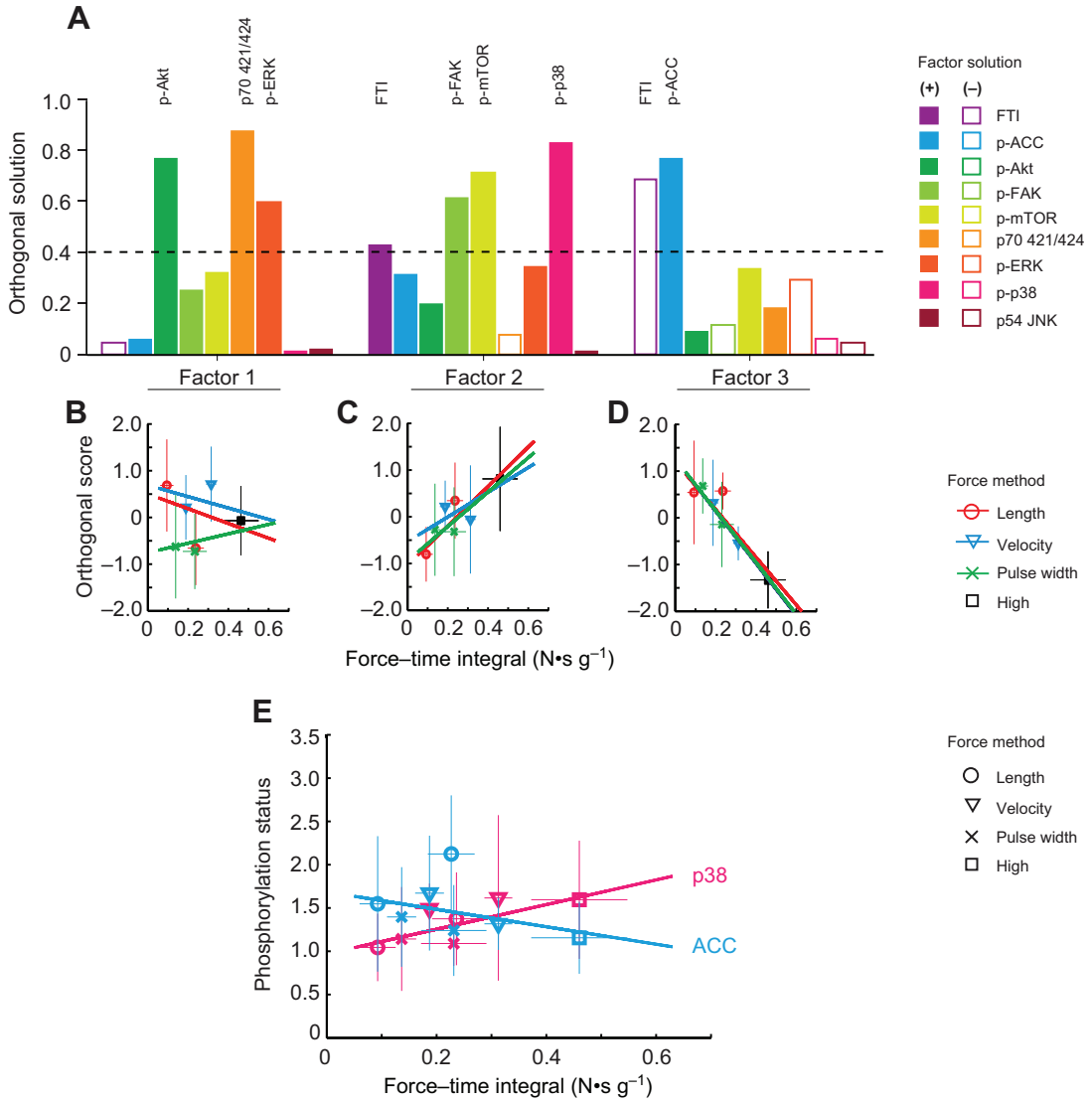

Fig. 8. (A) Component contributions to the three factors identified by factor analysis of the force–method data set. Bars with a positive (filled) or negative (open) loading greater than 0.4 indicate primary components of that factor. Regression plots of Factor 1 (B), Factor 2 (C) and Factor 3 (D) against FTI. (E) Regression of major components of factor 2 and 3 against FTI (p38: P=0.043; ACC: P=0.21).

observations in *Drosophila* that p38 is a positive regulator of mTOR through TSC1/2-dependent mechanisms (Cully et al., 2010), potentially by promoting interaction of TSC1/2 and 14-3-3 (Hernández et al., 2011). The persistence of the p38–mTOR module even under high metabolic stress in the HDC protocols suggests that activation of a force-related growth pathway can occur simultaneous with activation of AMPK.

Implications for voluntary exercise

Extremely transient bouts of muscle overload are sufficient to drive persistent changes in muscle growth (Adams et al., 2004; Baar and Esser, 1999; Leslie and Downes, 2004). A training regimen such as HDC-long, consisting of just 20 s of activation every second day is sufficient to induce hypertrophy and changes in gene expression (Adams et al., 2004; Baar and Esser, 1999), while only 10 s of daily stimulation is sufficient to prevent denervation-induced atrophy (Dow et al., 2004). Signaling events during transient force generation must encode information required to initiate an appropriate and persistent response.

Although we found a p38–mTOR signaling module correlated with FTI, several of the strongly induced phosphorylations, including ERK and JNK, were independent of stimulation conditions, and may reflect the complete activation of muscle achieved by HFES. Voluntary exercise is performed under very different constraints than electrical stimulation. During voluntary exercise, successful repetition requires activation of a subset of fibers to match the target weight, even as those fibers fatigue. During voluntary exercise, repetition may promote recruitment of the fast IIx or IIb fibers more sensitive to growth stimuli (Chalmers et al., 1992). If so, then exercise regimens that induce contractile failure rapidly may promote hypertrophy by driving more complete recruitment of muscle fibers, rather than by driving a different signaling program. Low-force exercise under blood flow occlusion is thought to exert its hypertrophic benefits by increasing fiber recruitment, specifically fast fibers (Wernbom et al., 2008). Burd et al. found that performing low force exercise to fatigue (failure) induced greater cell signaling and changes in protein synthesis than high force exercise to fatigue (Burd et al., 2010). Contraction-induced signaling integrates

potentially conflicting force and metabolic stimuli to allow simultaneous increase in AMPK activity (ACC phosphorylation) along with p38 and mTORC1 signaling, despite the negative feedback between these pathways.

LIST OF SYMBOLS AND ABBREVIATIONS

ACC	acetyl-CoA carboxylase
AICAR	5-aminoimidazole-4-carboxamide ribonucleotide
AMPK	AMP-activated protein kinase
APF	average peak force
DC	duty cycle
FTI	force–time interval
HDC	high duty cycle
HFC	high force contraction
HFES	high-frequency electrical stimulation
I_0	current
L	length
L_0	optimum muscle length
LDC	low duty cycle
MAPK	mitogen-activated protein kinase
mTOR	mammalian target of rapamycin
P_0	maximal isometric tension
P_t	maximal twitch force
PW	pulse width
StimDur	stimulation duration
TA	tibialis anterior
V	velocity
IOD	integrated optical density

ACKNOWLEDGEMENTS

The authors would like to acknowledge the technical assistance of Ronodeep Srimani.

AUTHOR CONTRIBUTIONS

J.A.R. contributed to the design and execution of the study, interpretation of the findings, and writing of the manuscript. T.J.B. contributed to the design of the study, interpretation of the findings, and writing of the manuscript.

COMPETING INTERESTS

No competing interests declared.

FUNDING

This work was supported by the National Institutes of Health (NIH) [DC005017]. The NIH had no role in the design, performance or interpretation of the study, nor in the decision to publish. Deposited in PMC for release after 12 months.

REFERENCES

Adams, G. R., Caiozzo, V. J., Haddad, F. and Baldwin, K. M. (2002). Cellular and molecular responses to increased skeletal muscle loading after irradiation. *Am. J. Physiol.* **283**, C1182-C1195.

Adams, G. R., Cheng, D. C., Haddad, F. and Baldwin, K. M. (2004). Skeletal muscle hypertrophy in response to isometric, lengthening, and shortening training bouts of equivalent duration. *J. Appl. Physiol.* **96**, 1613-1618.

Aikawa, R., Nagai, T., Kudoh, S., Zou, Y., Tanaka, M., Tamura, M., Akazawa, H., Takano, H., Nagai, R. and Komuro, I. (2002). Integrins play a critical role in mechanical stress-induced p38 MAPK activation. *Hypertension* **39**, 233-238.

Baar, K. and Esser, K. (1999). Phosphorylation of p70(S6k) correlates with increased skeletal muscle mass following resistance exercise. *Am. J. Physiol.* **276**, C120-C127.

Barclay, C. J., Arnold, P. D. and Gibbs, C. L. (1995). Fatigue and heat production in repeated contractions of mouse skeletal muscle. *J. Physiol.* **488**, 741-752.

Bodine, S. C., Stitt, T. N., Gonzalez, M., Kline, W. O., Stover, G. L., Bauerlein, R., Zlotchenko, E., Scrimgeour, A., Lawrence, J. C., Glass, D. J. et al. (2001). Akt/mTOR pathway is a crucial regulator of skeletal muscle hypertrophy and can prevent muscle atrophy *in vivo*. *Nat. Cell Biol.* **3**, 1014-1019.

Bolster, D. R., Crozier, S. J., Kimball, S. R. and Jefferson, L. S. (2002). AMP-activated protein kinase suppresses protein synthesis in rat skeletal muscle through down-regulated mammalian target of rapamycin (mTOR) signaling. *J. Biol. Chem.* **277**, 23977-23980.

Burd, N. A., West, D. W., Staples, A. W., Atherton, P. J., Baker, J. M., Moore, D. R., Holwerda, A. M., Parise, G., Rennie, M. J., Baker, S. K. et al. (2010). Low-load high volume resistance exercise stimulates muscle protein synthesis more than high-load low volume resistance exercise in young men. *PLoS ONE* **5**, e12033.

Burkholder, T. J., Fingado, B., Baron, S. and Lieber, R. L. (1994). Relationship between muscle fiber types and sizes and muscle architectural properties in the mouse hindlimb. *J. Morphol.* **221**, 177-190.

Challiss, R. A., Blackledge, M. J., Shoubridge, E. A. and Radda, G. K. (1989). A gated 31P-n.m.r. study of bioenergetic recovery in rat skeletal muscle after tetanic contraction. *Biochem. J.* **259**, 589-592.

Chalmers, G. R., Roy, R. R. and Edgerton, V. R. (1992). Variation and limitations in fiber enzymatic and size responses in hypertrophied muscle. *J. Appl. Physiol.* **73**, 631-641.

Cully, M., Genevet, A., Warne, P., Treins, C., Liu, T., Bastien, J., Baum, B., Tapon, N., Leevers, S. J. and Downward, J. (2010). A role for p38 stress-activated protein kinase in regulation of cell growth via TORC1. *Mol. Cell. Biol.* **30**, 481-495.

Deshmukh, A. S., Treebak, J. T., Long, Y. C., Viollet, B., Wojtaszewski, J. F. and Zierath, J. R. (2008). Role of adenosine 5′-monophosphate-activated protein kinase subunits in skeletal muscle mammalian target of rapamycin signaling. *Mol. Endocrinol.* **22**, 1105-1112.

Dow, D. E., Cederna, P. S., Hassett, C. A., Kostrominova, T. Y., Faulkner, J. A. and Dennis, R. G. (2004). Number of contractions to maintain mass and force of a denervated rat muscle. *Muscle Nerve* **30**, 77-86.

Fenn, W. O. and Latchford, W. B. (1933). The effect of muscle length on the energy for maintenance of tension. *J. Physiol.* **80**, 213-219.

Flück, M., Carson, J. A., Gordon, S. E., Ziemiecki, A. and Booth, F. W. (1999). Focal adhesion proteins FAK and paxillin increase in hypertrophied skeletal muscle. *Am. J. Physiol.* **277**, C152-C162.

Garma, T., Kobayashi, C., Haddad, F., Adams, G. R., Bodell, P. W. and Baldwin, K. M. (2007). Similar acute molecular responses to equivalent volumes of isometric, lengthening, or shortening mode resistance exercise. *J. Appl. Physiol.* **102**, 135-143.

Goodman, C. A., Frey, J. W., Mabrey, D. M., Jacobs, B. L., Lincoln, H. C., You, J. S. and Hornberger, T. A. (2011). The role of skeletal muscle mTOR in the regulation of mechanical load-induced growth. *J. Physiol.* **589**, 5485-5501.

Hentzen, E. R., Lahey, M., Peters, D., Mathew, L., Barash, I. A., Fridén, J. and Lieber, R. L. (2006). Stress-dependent and -independent expression of the myogenic regulatory factors and the MARP genes after eccentric contractions in rats. *J. Physiol.* **570**, 157-167.

Hernández, G., Lal, H., Fidalgo, M., Guerrero, A., Zalvide, J., Force, T. and Pombo, C. M. (2011). A novel cardioprotective p38-MAPK/mTOR pathway. *Exp. Cell Res.* **317**, 2938-2949.

Holm, L., van Hall, G., Rose, A. J., Miller, B. F., Doessing, S., Richter, E. A. and Kjaer, M. (2010). Contraction intensity and feeding affect collagen and myofibrillar protein synthesis rates differently in human skeletal muscle. *Am. J. Physiol.* **298**, E257-E269.

Hornberger, T. A. and Chien, S. (2005). Mechanical stimuli and nutrients regulate rapamycin-sensitive signaling through distinct mechanisms in skeletal muscle. *J. Cell. Biochem.* **97**, 1207-1216. PubMed

Hornberger, T. A., Armstrong, D. D., Koh, T. J., Burkholder, T. J. and Esser, K. A. (2005). Intracellular signaling specificity in response to uniaxial vs. multiaxial stretch: implications for mechanotransduction. *Am. J. Physiol.* **288**, C185-C194.

Huxley, A. F. (1957). Muscle structure and theories of contraction. *Prog. Biophys. Biophys. Chem.* **7**, 255-318.

Inoki, K., Li, Y., Zhu, T., Wu, J. and Guan, K. L. (2002). TSC2 is phosphorylated and inhibited by Akt and suppresses mTOR signalling. *Nat. Cell Biol.* **4**, 648-657.

Lal, H., Verma, S. K., Smith, M., Guleria, R. S., Lu, G., Foster, D. M. and Dostal, D. E. (2007). Stretch-induced MAP kinase activation in cardiac myocytes: differential regulation through beta1-integrin and focal adhesion kinase. *J. Mol. Cell. Cardiol.* **43**, 137-147.

Lantier, L., Mounier, R., Leclerc, J., Pende, M., Foretz, M. and Viollet, B. (2010). Coordinated maintenance of muscle cell size control by AMP-activated protein kinase. *FASEB J.* **24**, 3555-3561.

Lemieux, K., Konrad, D., Klip, A. and Marette, A. (2003). The AMP-activated protein kinase activator AICAR does not induce GLUT4 translocation to transverse tubules but stimulates glucose uptake and p38 mitogen-activated protein kinases alpha and beta in skeletal muscle. *FASEB J.* **17**, 1658-1665.

Leslie, N. R. and Downes, C. P. (2004). PTEN function: how normal cells control it and tumour cells lose it. *Biochem. J.* **382**, 1-11.

Lluís, F., Perdiguero, E., Nebreda, A. R. and Muñoz-Cánoves, P. (2006). Regulation of skeletal muscle gene expression by p38 MAP kinases. *Trends Cell Biol.* **16**, 36-44.

Lo, S., Russell, J. C. and Taylor, A. W. (1970). Determination of glycogen in small tissue samples. *J. Appl. Physiol.* **28**, 234-236.

Ma, L., Chen, Z., Erdjument-Bromage, H., Tempst, P. and Pandolfi, P. P. (2005). Phosphorylation and functional inactivation of TSC2 by Erk implications for tuberous sclerosis and cancer pathogenesis. *Cell* **121**, 179-193.

Maarbjerg, S. J., Jørgensen, S. B., Rose, A. J., Jeppesen, J., Jensen, T. E., Treebak, J. T., Birk, J. B., Schjerling, P., Wojtaszewski, J. F. and Richter, E. A. (2009). Genetic impairment of AMPKalpha2 signaling does not reduce muscle glucose uptake during treadmill exercise in mice. *Am. J. Physiol.* **297**, E924-E934.

Martineau, L. C. and Gardiner, P. F. (2001). Insight into skeletal muscle mechanotransduction: MAPK activation is quantitatively related to tension. *J. Appl. Physiol.* **91**, 693-702.

Miyazaki, M. and Esser, K. A. (2009). Cellular mechanisms regulating protein synthesis and skeletal muscle hypertrophy in animals. *J. Appl. Physiol.* **106**, 1367-1373.

Nader, G. A. and Esser, K. A. (2001). Intracellular signaling specificity in skeletal muscle in response to different modes of exercise. *J. Appl. Physiol.* **90**, 1936-1942.

Potma, E. J., Stienen, G. J., Barends, J. P. and Elzinga, G. (1994). Myofibrillar ATPase activity and mechanical performance of skinned fibres from rabbit psoas muscle. *J. Physiol.* **474**, 303-317.

Pullen, N. and Thomas, G. (1997). The modular phosphorylation and activation of p70s6k. *FEBS Lett.* **410**, 78-82.

Russ, D. W. (2008). Active and passive tension interact to promote Akt signaling with muscle contraction. *Med. Sci. Sports Exerc.* **40**, 88-95.

Sabourin, L. A. and Rudnicki, M. A. (2000). The molecular regulation of myogenesis. *Clin. Genet.* **57**, 16-25.

Spangenburg, E. E. (2009). Changes in muscle mass with mechanical load: possible cellular mechanisms. *Appl. Physiol. Nutr. Metab.* **34**, 328-335.

Spangenburg, E. E., Le Roith, D., Ward, C. W. and Bodine, S. C. (2008). A functional insulin-like growth factor receptor is not necessary for load-induced skeletal muscle hypertrophy. *J. Physiol.* **586**, 283-291.
Stephenson, D. G., Stewart, A. W. and Wilson, G. J. (1989). Dissociation of force from myofibrillar MgATPase and stiffness at short sarcomere lengths in rat and toad skeletal muscle. *J. Physiol.* **410**, 351-366.
Thomson, D. M., Fick, C. A. and Gordon, S. E. (2008). AMPK activation attenuates S6K1, 4E-BP1, and eEF2 signaling responses to high-frequency electrically stimulated skeletal muscle contractions. *J. Appl. Physiol.* **104**, 625-632.
Wang, X., Flynn, A., Waskiewicz, A. J., Webb, B. L., Vries, R. G., Baines, I. A., Cooper, J. A. and Proud, C. G. (1998). The phosphorylation of eukaryotic initiation factor eIF4E in response to phorbol esters, cell stresses, and cytokines is mediated by distinct MAP kinase pathways. *J. Biol. Chem.* **273**, 9373-9377.
Wernbom, M., Augustsson, J. and Raastad, T. (2008). Ischemic strength training: a low-load alternative to heavy resistance exercise? *Scand. J. Med. Sci. Sports* **18**, 401-416.
Wong, T. S. and Booth, F. W. (1990). Protein metabolism in rat tibialis anterior muscle after stimulated chronic eccentric exercise. *J. Appl. Physiol.* **69**, 1718-1724.
Wretman, C., Lionikas, A., Widegren, U., Lännergren, J., Westerblad, H. and Henriksson, J. (2001). Effects of concentric and eccentric contractions on phosphorylation of MAPK(erk1/2) and MAPK(p38) in isolated rat skeletal muscle. *J. Physiol.* **535**, 155-164.
Wu, Z., Woodring, P. J., Bhakta, K. S., Tamura, K., Wen, F., Feramisco, J. R., Karin, M., Wang, J. Y. and Puri, P. L. (2000). p38 and extracellular signal-regulated kinases regulate the myogenic program at multiple steps. *Mol. Cell. Biol.* **20**, 3951-3964.